PHOTONICS Research

Breathing dissipative soliton explosions in a bidirectional ultrafast fiber laser

Yı Zhou, ● Yu-Xuan Ren, ● Jiawei Shi, ● and Kenneth K. Y. Wong* ●

Department of Electrical and Electronic Engineering, The University of Hong Kong, Hong Kong, China
Corresponding author: kywong@eee.hku.hk

Soliton explosions, among the most exotic dynamics, have been extensively studied on parameter invariant stationary solitons. However, the explosion dynamics are still largely unexplored in breathing dissipative solitons as a dynamic solution to many nonlinear systems. Here, we report on the first observation of a breathing dissipative soliton explosion in a net-normal-dispersion bidirectional ultrafast fiber laser. The breathing soliton explosions could be stimulated by the soliton buildup process or alteration of polarization settings. Transient breathing soliton pairs with intensive repulsion that is sensitive to initial conditions can also be triggered by multiple soliton explosions in the soliton buildup process instead of being triggered by varying polarization settings. The high behavior similarity also exists in the breathing soliton buildup and explosion process owing to the common gain and loss modulation. In addition, dissipative rogue waves were detected in the breathing soliton explosion, and the collision of breathing soliton significantly enhanced the amplitude of rogue waves, which is characteristic of the breathing solitons in a bidirectional fiber laser. These results shed new insights into complex dissipative soliton dynamics. © 2020 Chinese Laser Press

https://doi.org/10.1364/PRJ.399998

1. INTRODUCTION

Solitons, as localized wave packets, result from the balance between nonlinearity and dispersion in the medium [1]. The stability of dissipative solitons stems from the dynamic attractors in dissipative systems. However, beyond fixed-point attractors, dissipative systems possess a wide range of nonlinear dynamics, including breathing and chaos [2]. Ultrafast fiber lasers, as typical dissipative systems, are particularly convenient for investigating versatile dissipative soliton dynamics, such as soliton buildup [3,4], soliton molecules [5,6], soliton explosions [7,8], rogue waves [9,10], and breathing solitons [11,12]. Among them, the soliton explosion is one of the fascinating localized structures in nonlinear systems, which has recently attracted significant research interest. In the soliton explosion regime, the dissipative soliton can explode into pieces under certain conditions and then recover to its original state later. Until now, numerous efforts have been devoted to investigating the soliton explosions. The earlier numerical result identified soliton explosions as a class of chaotic localized solutions of the complex cubic-quintic Ginzburg–Landau equation; further, high-order effects play important roles in the generation and characteristics of soliton explosions [13–15]. The first experimental evidence of soliton explosions was demonstrated in a Ti:sapphire laser and detected by a diffraction grating and an array of six detectors [16]. In 2015, the real-time dynamics of a soliton explosion was observed in a fiber laser by using the time-

stretch dispersive Fourier transform (TS-DFT) [7]; afterward, the experimental investigations on soliton explosions were greatly stimulated, including successive soliton explosions [17], vector incoherent soliton explosions [18], mutually ignited soliton explosions [19], etc.

However, the soliton explosions were limited in the stationary soliton regime and are still largely unexplored in the breathing dissipative soliton regime, which experiences periodic evolution of energy and spectra. Breathing dissipative solitons constitute an important context of nonlinear science and have been investigated in various physical systems [20–23]. On the other hand, breathing solitons have important practical applications, e.g., increase of the resolution in a dual-comb source [20]. Therefore, it is of fundamental significance to explore the condition to trigger a soliton explosion in breathing solitons, akin to stationary solitons. In addition, a soliton explosion is also related to the soliton collision, which has been theoretically predicted [24]. It is interesting to see whether a soliton explosion can be generated in a bidirectional ultrafast fiber laser in which counterpropagating breathing solitons collide in each roundtrip. Continuous interest in bidirectional mode-locking has also reinforced their practical application, such as ultrafast laser ring gyroscopes [25] and coherent dual-comb spectroscopy [26]. However, the lack of underlying research on soliton dynamics poses significant limitations to the development of bidirectional ultrafast laser applications. Therefore, it is

meaningful to investigate the exotic dynamics of breathing dissipative solitons in bidirectional ultrafast fiber lasers.

In previous reports of bidirectional fiber lasers, the soliton dynamics highly depends on the net cavity dispersion. The similarity in the spectrum and temporal characteristics has been observed in the buildup of stationary counterpropagating solitons in a net-normal dispersion bidirectional laser [27]. However, in the anomalous dispersion regime, the counterpropagating pulses experience independent buildup dynamics [28]. For the breathing soliton with net cavity dispersion close to zero, it is still worth exploring whether there exists behavior similarity in the transient instability such as the buildup and explosion process in counterpropagating solitons. The bidirectional breathing solitons colliding in each roundtrip may display different dynamics. In addition, the stable performance of bidirectional mode-locked fiber lasers is important for many applications. However, the soliton explosions and rogue waves associated with the inevitable soliton collision pose a negative influence on the performance of bidirectional fiber lasers, e.g., burnout of the fiber device. Therefore, more efforts need to be made in investigating the soliton dynamics of bidirectional mode-locked fiber lasers.

Currently, carbon nanotube (CNT) as a saturable absorber (SA) has been widely applied for mode-locking due to its advantages of the ultrafast recovery, cost-effective production, and ease of fiber integration. Besides, novel 2D materials, e.g., Ag_2S nanosheets and graphdiyne, have also been demonstrated as promising SA for the ultrafast fiber laser [29,30]. Here, we report on the first observation of the breathing dissipative soliton explosion in a CNT mode-locked bidirectional ultrafast fiber laser operating in the net-normal-dispersion regime. The breathing soliton explosion could be induced in the soliton buildup process or by varying the polarization setting. Transient breathing soliton pairs with intensive repulsion that is sensitive to the initial condition can also be triggered by multiple soliton explosions in the soliton buildup process rather than the polarization. In the transient instability regime, the breathing solitons from the clockwise (CW) and counterclockwise (CCW) directions possess high behavior similarity owing to the common gain/loss modulation [27]. Moreover, rogue waves (RWs) are observed during breathing soliton explosions. The collision of breathing solitons significantly enhances the amplitude of RWs that characterize the breathing soliton in the bidirectional fiber laser in contrast with the unidirectional fiber laser. These results shed light on further understanding of the nonlinear dynamics of a breathing soliton explosion in dissipative systems.

2. EXPERIMENTAL SETUP

The experimental setup for bidirectional breathing soliton generation was a passively mode-locked Er-doped fiber laser based on the CNT as the saturable absorber (Fig. 1). The fiber cavity included an 11.5 m erbium-doped fiber (EDF, M12-980-125) with a group-velocity dispersion (GVD) parameter of about 18.5 ps^2/km and a 3.7 m SM28-e fiber with a GVD parameter of $\sim$ −22 ps^2/km, operated in a normal dispersion regime with a net cavity dispersion of $\sim$0.13 ps^2. The length of the whole laser cavity was around 15.2 m, suggesting a repetition rate of
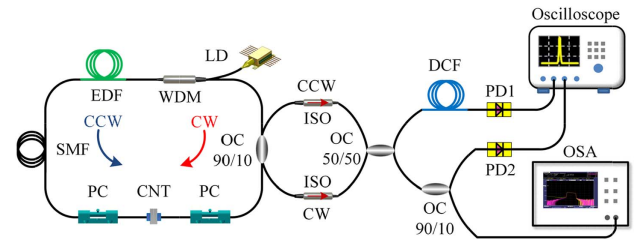

Fig. 1. Schematic illustration of the fiber laser cavity and measurement setup.

13.2 MHz. Two polarization controllers were inserted into the cavity to optimize the polarization state. A coupler with a 10/90 splitting ratio was used to extract 10% of pulse power in each direction for measurement. A 50/50 coupler combined counterpropagating pulses for consistent and synchronous analysis. A proper delay was introduced at the input ports of the 50/50 coupler to avoid temporal overlap. The temporal information was detected by a 20 GHz photodiode (PD2, Agilent 83440 C) and digitized by a 20 GHz real-time oscilloscope (Lecroy SDA 820Zi-B), while the spectra were detected by an optical spectrum analyzer (OSA, Yokogawa AQ6370D) and TS-DFT technique simultaneously. The DFT branch was composed of a spool of dispersion compensating fiber (DCF) with −577 ps/nm dispersion and detected by a 12 GHz photodiode (PD1, New Focus 1544-B). The temporal and spectral resolution was 50 ps and 0.17 nm, respectively [31].

3. RESULTS AND DISCUSSION

The laser operates in different states when the pump power is changing. At the particular polarization setting, the breathing dissipative solitons can be directly generated in the mode-locking buildup process at a pump of 15 mW. The stable breathing solitons are shown in Fig. 2 at a pump power of 17.5 mW. The solitons spectra for both CCW and CW pose the same center wavelength of 1595 nm [Fig. 2(a)] but with
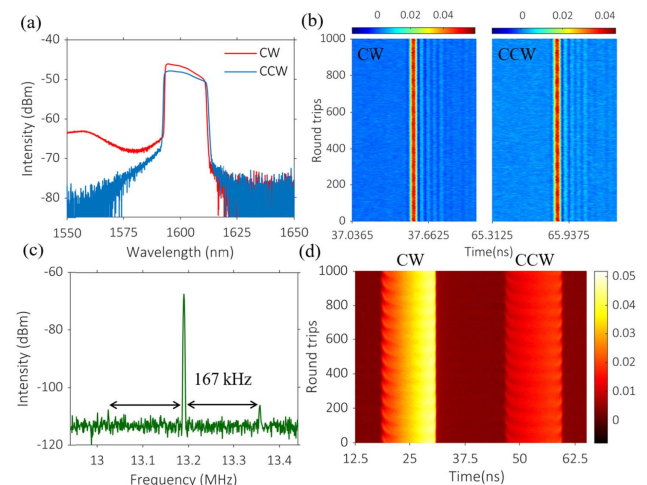

Fig. 2. Stable breathing soliton state. (a) Average spectra recorded by an OSA. (b) Temporal evolution. (c) RF spectrum. (d) Spectral evolution.

distinguishable bandwidth (18.7 nm for CCW pulse, and 15 nm for the CW pulse). The CW pulse possesses higher energy and amplified spontaneous emission (ASE) noise that attributes to the asymmetric pump structure of the EDF. The CW soliton separates from the CCW soliton with a constant temporal distance of 28.3 ns, suggesting an identical repetition rate in both directions [Fig. 2(b)]. The radio frequency (RF) spectrum [Fig. 2(c)] suggests a frequency difference of 167 kHz between the satellite component (induced by the breathing) and the fundamental repetition frequency of 13.19 MHz, which agrees well with the breath period of 79 roundtrips (RTs). Furthermore, there is only one fundamental frequency and satellite peak frequency, which further demonstrates the synchronization and the same breathing period of solitons in both directions. Figure 2(d) shows the spectrum evolution of counterpropagating solitons with clear breathing behavior corresponding to the same breathing period of 79 RTs. It should be noted that the breathing solitons of opposite propagating directions collide in the cavity every roundtrip. The collision point in the cavity is inferred as the location of the CNT, which leads to a good temporal synchronization of counterpropagating pulses. The CNT produces equivalent loss modulation for the solitons as the common transmission path through the CNT simultaneously. Therefore, the bidirectional breathing dissipative solitons exhibit similar performance in this laser system, e.g., the same breathing period, spectral center wavelength, and repetition rate.

The breathing soliton explosion could be triggered in the soliton buildup process or through polarization manipulation, different from the one by decreasing pump power [20]. The buildup process of breathing solitons suggests the frequent occurrence of multiple soliton explosions. The number of soliton explosions can also be increased by increasing the initial pump power for mode-locking. Figures 3(a) and 3(b) show the temporal evolution along with the CW and CCW directions, respectively. Note that the seed pulses always occur in pairs, and the soliton buildup and explosion behavior along both

directions happen almost simultaneously. The characteristic temporal shift appears in the soliton explosion process [Figs. 3(a) and 3(b)] [7,18]. Although the soliton energy varied dramatically during the evolution, the temporal separation of counterpropagating solitons remains constant. The breathing soliton buildup in both directions also suggests similar spectrum evolution [Fig. 3(c)] from the background noise. As the energy dramatically increases, the spectrum broadens until quasi-stable mode-locking is reached in the breathing soliton. In the soliton explosion regime, an abrupt spectral collapse occurs during the breathing soliton mode-locking, and the periodic spectral evolution in dual directions is disrupted by wide and chaotic spectra. The duration of the soliton explosion in both directions is about 900 RTs; then, the solitons recover quasi-stable breathing operation. The energy (integration of spectral density) evolution follows the same trend for counterpropagating breathing solitons [Fig. 3(d)]. In both the buildup and explosion processes, the soliton energy exhibits a dramatic increase and fall-off, and then reverts to the oscillating state. The apparent energy oscillation demonstrates the breathing dynamics of dissipative solitons [inset in Fig. 3(d)].

Figure 4 shows two typical intermittent breathing soliton explosions induced by the soliton buildup at a mode-locking pump power of 26 mW. Figures 4(a) and 4(b) show the spectral evolution of breathing soliton explosion with five aperiodic and intermittent explosion events. Specifically, when an explosion occurs, the spectrum experienced a complete collapse and final return to the breathing soliton state. This feature is significantly different from the multiple soliton explosion that occurs in a nonlinear amplifying loop mirror (NALM) mode-locked fiber laser, for which the spectrally broad dissipative soliton partially collapses into a narrower spectrum with enhanced amplitude [7]. In addition, the spectrum evolution for counterpropagating breathing solitons is quite similar in the multiple soliton explosion. Figures 4(c) and 4(d) show the soliton energy evolution corresponding to the spectra in Figs. 4(a) and 4(b), respectively. The energy evolution suggests that none of the soliton explosions would be identical for the breathing soliton explosion events. For the explosion in the dashed rectangle of Fig. 4(d), the soliton energy periodically oscillating characterizes the breathing behavior before the soliton explosion takes place. Then, the soliton energy dramatically increases, followed by a sharp decrease to a low value, which is smaller than that of the quasi-stable state, suggesting a total collapse of the spectrum. The second pair of a fast rise and decrease of the soliton energy corresponds to the recovery of the breathing soliton, and the similar feature of the mode-locking rebuilding has been observed in the net normal dispersion mode-locked fiber laser [32]. For another explosion in the dashed rectangle of Fig. 4(c), the second swift rise and decrease in the soliton energy is similar to the explosion event shown by the dashed rectangle in Fig. 4(d). However, the difference is that, when the soliton explosion occurs, the soliton energy first dramatically increases, followed by a dip (partial decrease) in the energy; then, soliton energy rapidly recovers and eventually decreases to a low value that corresponds to the total spectrum collapse. Figures 4(e) and 4(f) show the spectrum evolution corresponding to the dashed rectangle in Figs. 4(c) and 4(d), suggesting
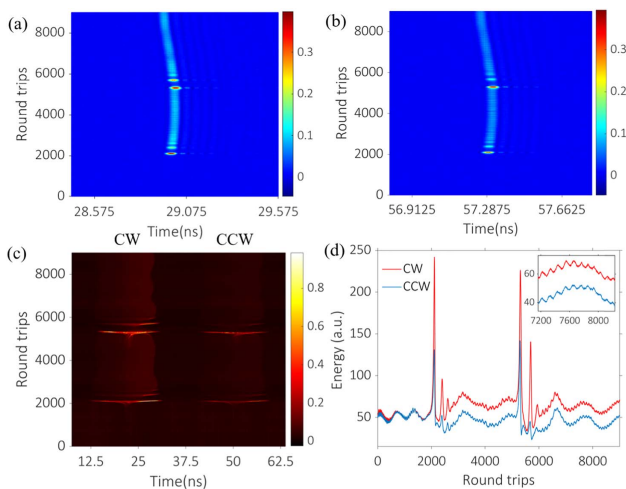

Fig. 3. Buildup and soliton explosion of breathing soliton. Temporal evolution in (a) CW and (b) CCW directions. (c) Shot-to-shot spectral evolution. (d) Energy evolution.
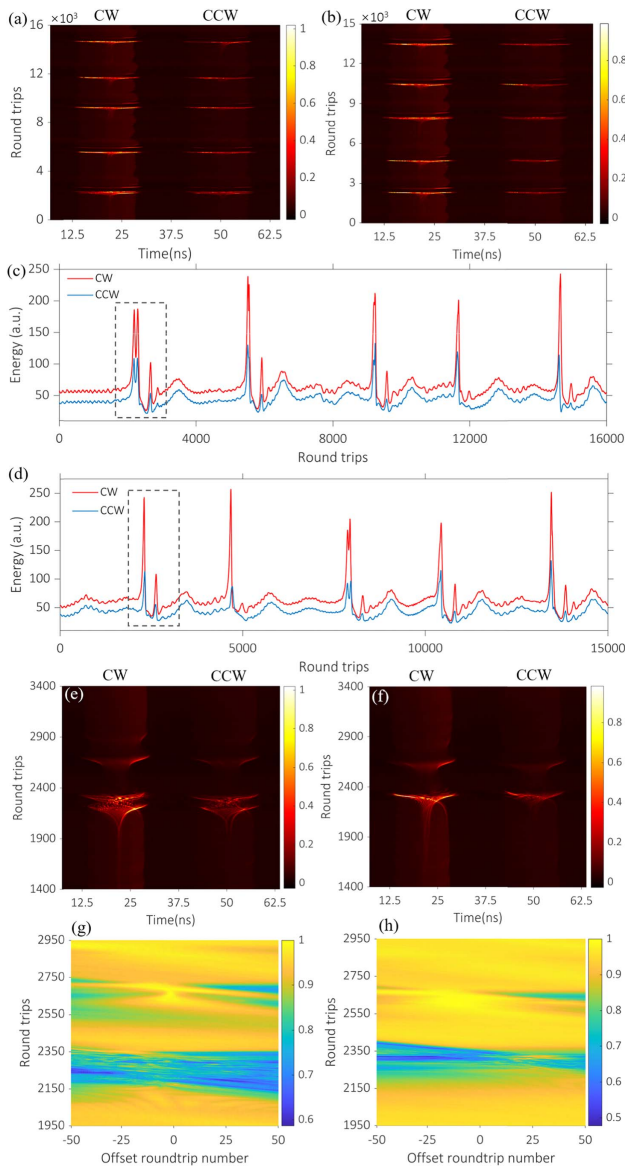
Fig. 4. Intermittent soliton explosions in breathing soliton buildup process. (a), (b) Spectral evolution of two typical intermittent breathing soliton explosions. (c), (d) Energy evolution corresponding to (a) and (b), respectively. (e), (f) Spectral evolution corresponding to dashed rectangle in (c) and (d), respectively. (g), (h) Spectral cross-correlation map corresponding to (e) and (f), respectively.

distinguishable soliton explosion behavior for different soliton energy evolution dynamics.

The spectral behavior for the breathing dissipative solitons [Figs. 4(e) and 4(f)] was further compared through cross-correlation [Figs. 4(g) and 4(h)] between single-shot spectra from opposite directions. For every roundtrip with index N from 1950 to 2950 propagating in the CW direction, the spectrum cross-correlation with RTs from $N - 50$ to $N + 50$ in the CCW direction is calculated. In Figs. 4(g) and 4(h), the cross-correlation magnitude reveals similarity in the two single-shot spectra from opposite directions. Notably, the spectra show an insignificant change in the quasi-stable state. For each

roundtrip from the CW direction, many RTs from the CCW direction share a high spectral similarity. The high spectral similarity could also be found in the most variant part of the soliton explosion. In contrast with the behavior similarity in the stationary soliton process [27], the behavior similarity of solitons in both directions also exists in the breathing soliton explosion process. This finding has been further corroborated by the observation of the energy and spectrum evolution in both directions for more soliton explosion events.

In addition, transient breathing soliton pairs with intensive repulsion can also be triggered by multiple soliton explosions in the soliton buildup process. Figure 5 shows the transient breathing soliton pair generation induced by soliton explosion corresponding to mode-locking pump power of 20 mW. Figures 5(a) and 5(b) show the temporal and spectral evolution along with CW and CCW directions, respectively. When soliton explosion occurs, a weak leading pulse and a stronger intensity trailing pulse are generated in the breathing soliton recovery process in the CW and CCW directions. However, the transient breathing soliton pair is not stable. The dual breathing solitons repel each other once they are generated. The leading pulse becomes weaker and finally disappears, resulting from the mode-locking mechanism that imposes the intensity-dependent transmission coefficient on the pulses, namely, the weak pulse undergoes higher loss. The corresponding temporal separation of leading and trailing pulses is 0.7 ns between solitons in both directions when leading pulses disappear at RTs of 16,080 [Fig. 5(a)]. Figure 5(c) is a closeup view of Fig. 5(b) to show the weak leading pulse possesses more obvious breathing behavior compared with the stronger trailing pulse. In the dual-soliton repulsive process, the spectrum of the leading pulse gradually narrows and disappears at RT of 16,080, and the spectrum of the trailing pulse gradually widens. The counterpropagating solitons energy evolution follows the same trend [Fig. 5(d)]. The inset in Fig. 5(d) further suggests obvious energy oscillation in the breathing dynamics of bidirectional solitons.

Besides the buildup process, the breathing soliton explosion can also be triggered by varying the polarization at critical mode-locking pump power (Fig. 6). In contrast with a frequent soliton explosion in the buildup process, the explosion of the breathing soliton only takes place once in a long duration of 84,000 RTs [Fig. 6(a)]. A closeup view [Fig. 6(b)] shows better detail of the soliton explosion marked by the dashed rectangle in Fig. 6(a). The dashed rectangle in Fig. 6(b) suggests a narrow peak generated in the breathing soliton spectrum, which indicates the soliton will enter the chaotic soliton explosion regime, consistent with the theoretical prediction [33]. After the recovery of stable breathing, the narrow peak in the spectrum disappears. Three representative real-time spectra at different RTs are given, corresponding to the stages of stable breathing soliton mode-locking [Fig. 6(c)], i.e., the soliton explosion when the soliton energy rises to maximum [Fig. 6(d)] and soliton energy decreases to the valley [Fig. 6(e)], respectively. These transient spectra further demonstrate the behavioral similarity of counterpropagating solitons in the soliton explosion process.

In the breathing soliton explosion, extremely high-amplitude waves have also been observed, suggesting the
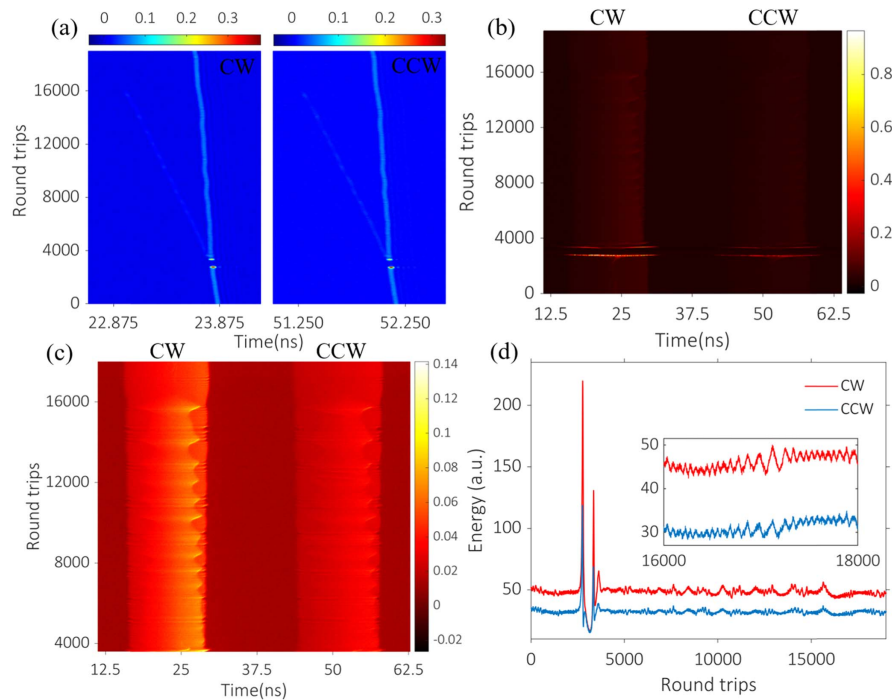
Fig. 5. Transient breathing soliton pair induced by soliton explosion. (a) Temporal evolution in CW and CCW directions. (b) Shot-to-shot spectral evolution. (c) Zoom-in plot of (b). (d) Energy evolution.
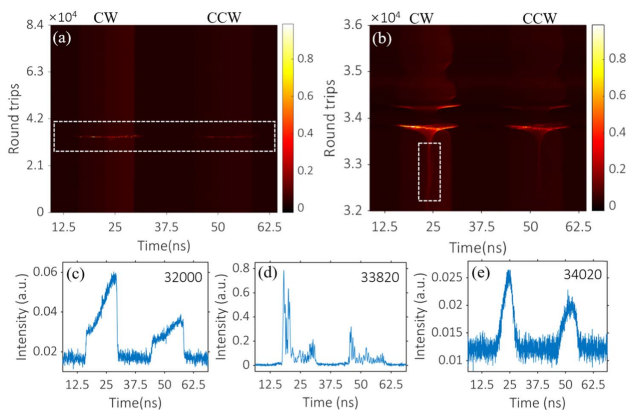

Fig. 6. Breathing soliton explosion maneuvered by polarization. (a) Spectral evolution. (b) Zoom-in plot of dashed rectangle in (a). (c)–(e) Example spectra at RTs of 32,000, 33,820, and 34,020.

Fig. 7. Intensity histogram of the breathing soliton explosion. Dashed line indicates the SWH.

emergence of optical rogue waves (RWs) in the soliton explosion. This is corroborated by recording the shot-to-shot DFT stretched pulse sequence. The statistical histogram for the amplitude fluctuations in the breathing soliton explosion for 80,000 peak amplitudes suggests a long-tail distribution (Fig. 7), and the majority amplitude events are concentrated at lower intensity, while the extremely high amplitude events appear rather rarely. The significant wave height (SWH), defined as the average amplitude of the highest third of waves, is calculated to be ∼0.079 V (dashed line in Fig. 7); further, the highest recorded amplitude is about ∼0.98 V, which reaches 12.4 times that of the SWH. It should be noted that
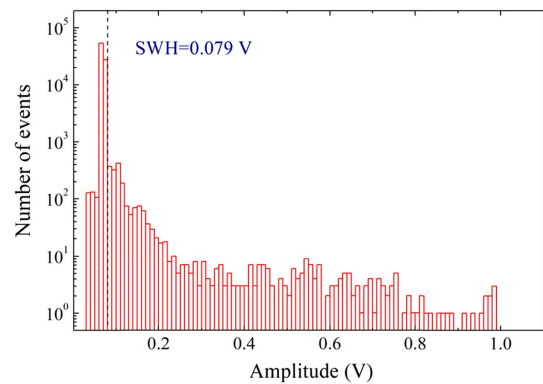
each recorded amplitude is the highest value of solitons along both directions. The statistical criterion to evaluate RW generation is that the highest measured amplitude should be larger than twice the SWH. Therefore, it could be confirmed that RWs have been generated in the breathing soliton explosion. In some typical RWs generation events in fiber lasers, the maximum optical amplitude exceeds ∼4 times the SWH [18,20,34]. The highest amplitude events of around 12 times the SWH in this experiment suggest a dramatic increase in the amplitude of the extreme event owing to the collision of bidirectional breathing solitons in the CNT, consistent with theoretical research [35,36].

In this CNT-based bidirectional mode-locked fiber laser, counterpropagating breathing solitons share the same

dispersion and optical path but in the opposite direction. Meanwhile, the breathing bidirectional solitons pass through the CNT together with the same cavity loss and similar gain profile. Therefore, the solitons in the buildup process and soliton explosion regime naturally synchronize in time and possess high behavior similarity. The breathing soliton explosion could be induced by the buildup process or variation in polarization and is also related to the breathing soliton collision in the CNT. In the soliton buildup process or polarization variation, the system parameter experiences a dramatic change, further affecting the energy evolution and nonlinearity in the cavity for each soliton. Therefore, breathing solitons encounter instability and explosion, and then recovery to a breathing soliton state due to the self-stabilization. In addition, the more complex multisoliton dynamics like the formation of a soliton molecule in a bidirectional ultrafast fiber laser can be further explored by fine design of the net cavity dispersion and adjustment of the pump power.

4. CONCLUSION

In conclusion, the breathing dissipative soliton explosion can be triggered by the soliton buildup process or varying polarization settings in a CNT-based bidirectional ultrafast fiber laser. The transient breathing soliton pairs with intensive repulsion can also be observed in multiple soliton explosion processes. The counterpropagating breathing solitons exhibit high behavior similarity in the soliton buildup and explosion process owing to common gain/loss modulation. The RWs were also generated in our fiber laser owing to the breathing soliton explosion, and the amplitude of RW was significantly enhanced by the collision of the bidirectional breathing soliton. We anticipate our work will stimulate further studies of breathing soliton explosions and RWs in various dissipative systems.

Disclosures. The authors declare no conflicts of interest.

REFERENCES

1. N. Akhmediev and A. Ankiewicz, *Solitons, Nonlinear Pulses and Beams* (Chapman and Hall, 1997).
2. P. Grelu and N. Akhmediev, "Dissipative solitons for mode-locked lasers," Nat. Photonics **6**, 84–92 (2012).
3. G. Herink, B. Jalali, C. Ropers, and D. Solli, "Resolving the buildup of femtosecond mode-locking with single-shot spectroscopy at 90 MHz frame rate," Nat. Photonics **10**, 321–326 (2016).
4. J. Peng, M. Sorokina, S. Sugavanam, N. Tarasov, D. V. Churkin, S. K. Turitsyn, and H. Zeng, "Real-time observation of dissipative soliton formation in nonlinear polarization rotation mode-locked fibre lasers," Commun. Phys. **1**, 20 (2018).
5. G. Herink, F. Kurtz, B. Jalali, D. R. Solli, and C. Ropers, "Real-time spectral interferometry probes the internal dynamics of femtosecond soliton molecules," Science **356**, 50–54 (2017).
6. X. M. Liu, X. K. Yao, and Y. D. Cui, "Real-time observation of the buildup of soliton molecules," Phys. Rev. Lett. **121**, 023905 (2018).
7. A. F. J. Runge, N. G. R. Broderick, and M. Erkintalo, "Observation of soliton explosions in a passively mode-locked fiber laser," Optica **2**, 36–39 (2015).
8. A. F. J. Runge, N. G. R. Broderick, and M. Erkintalo, "Dynamics of soliton explosions in passively mode-locked fiber lasers," J. Opt. Soc. Am. B **33**, 46–53 (2016).
9. D. R. Solli, C. Ropers, P. Koonath, and B. Jalali, "Optical rogue waves," Nature **450**, 1054–1057 (2007).
10. C. Lecaplain, P. Grelu, J. M. Soto-Crespo, and N. Akhmediev, "Dissipative rogue waves generated by chaotic pulse bunching in a mode-locked laser," Phys. Rev. Lett. **108**, 233901 (2012).
11. J. Peng, S. Boscolo, Z. Zhao, and H. Zeng, "Breathing dissipative solitons in mode-locked fiber lasers," Sci. Adv. **5**, eaax1110 (2019).
12. M. Liu, Z.-W. Wei, H. Li, T.-J. Li, A.-P. Luo, W.-C. Xu, and Z.-C. Luo, "Visualizing the 'invisible' soliton pulsation in an ultrafast laser," Laser Photon. Rev. **14**, 1900317 (2020).
13. J. M. Soto-Crespo, N. Akhmediev, and A. Ankiewicz, "Pulsating, creeping, and erupting solitons in dissipative systems," Phys. Rev. Lett. **85**, 2937–2940 (2000).
14. S. C. V. Latas and M. F. S. Ferreira, "Soliton explosion control by higher-order effects," Opt. Lett. **35**, 1771–1773 (2010).
15. S. V. Gurevich, C. Schelte, and J. Javaloyes, "Impact of high-order effects on soliton explosions in the complex cubic-quintic Ginzburg-Landau equation," Phys. Rev. A **99**, 061803 (2019).
16. S. T. Cundiff, J. M. Soto-Crespo, and N. Akhmediev, "Experimental evidence for soliton explosions," Phys. Rev. Lett. **88**, 073903 (2002).
17. M. Liu, A. P. Luo, Y. R. Yan, S. Hu, Y. C. Liu, H. Cui, Z. C. Luo, and W. C. Xu, "Successive soliton explosions in an ultrafast fiber laser," Opt. Lett. **41**, 1181–1184 (2016).
18. K. Krupa, K. Nithyanandan, and P. Grelu, "Vector dynamics of incoherent dissipative optical solitons," Optica **4**, 1239–1244 (2017).
19. Y. Yu, Z. C. Luo, J. Q. Kang, and K. K. Y. Wong, "Mutually ignited soliton explosions in a fiber laser," Opt. Lett. **43**, 4132–4135 (2018).
20. J. Peng and H. Zeng, "Experimental observations of breathing dissipative soliton explosions," Phys. Rev. Appl. **12**, 034052 (2019).
21. E. Lucas, M. Karpov, H. Guo, M. L. Gorodetsky, and T. J. Kippenberg, "Breathing dissipative solitons in optical microresonators," Nat. Commun. **8**, 736 (2017).
22. B. Kibler, J. Fatome, C. Finot, G. Millot, F. Dias, G. Genty, N. Akhmediev, and J. M. Dudley, "The Peregrine soliton in nonlinear fibre optics," Nat. Phys. **6**, 790–795 (2010).
23. M. Yu, J. K. Jang, Y. Okawachi, A. G. Griffith, K. Luke, S. A. Miller, X. Ji, M. Lipson, and A. L. Gaeta, "Breather soliton dynamics in microresonators," Nat. Commun. **8**, 14569 (2017).
24. O. Descalzi and H. R. Brand, "Collisions of non-explosive dissipative solitons can induce explosions," Chaos **28**, 075508 (2018).
25. M. Chernysheva, S. Sugavanam, and S. Turitsyn, "Real-time observation of the optical sagnac effect in ultrafast bidirectional fibre lasers," APL Photon. **5**, 016104 (2020).
26. T. Ideguchi, T. Nakamura, Y. Kobayashi, and K. Goda, "Kerr-lens modelocked bidirectional dual-comb ring laser for broadband dual-comb spectroscopy," Optica **3**, 748–753 (2016).
27. Y. Yu, C. Kong, B. Li, J. Kang, Y.-X. Ren, Z.-C. Luo, and K. K. Wong, "Behavioral similarity of dissipative solitons in an ultrafast fiber laser," Opt. Lett. **44**, 4813–4816 (2019).
28. I. Kudelin, S. Sugavanam, and M. Chernysheva, "Build-up dynamics in bidirectional soliton fibre laser," Photon. Res. **8**, 776–780 (2020).
29. J. J. Feng, X. H. Li, Z. J. Shi, C. Zhen, X. W. Li, D. Y. Leng, Y. M. Wang, J. Liu, and L. J. Zhu, "2D ductile transition metal chalcogenides (TMCs): a novel high-performance Ag₂S nanosheets for ultrafast photonics," Adv. Opt. Mater. **8**, 1901762 (2020).
30. Y. Zhao, P. L. Guo, X. H. Li, and Z. W. Jin, "Ultrafast photonics application of graphdiyne in optical communication region," Carbon **149**, 336–341 (2019).
31. K. K. Tsia, K. Goda, D. Capewell, and B. Jalali, "Performance of serial time-encoded amplified microscope," Opt. Express **18**, 10016–10028 (2010).
32. H. Chen, M. Liu, J. Yao, S. Hu, J. He, A. Luo, W. Xu, and Z. Luo, "Buildup dynamics of dissipative soliton in an ultrafast fiber laser with net-normal dispersion," Opt. Express **26**, 2972–2982 (2018).

33. Y. Du and X. Shu, "Dynamics of soliton explosions in ultrafast fiber lasers at normal-dispersion," Opt. Express **26**, 5564–5575 (2018).

34. M. Liu, T. Li, A. Luo, W. Xu, and Z. Luo, "'Periodic' soliton explosions in a dual-wavelength mode-locked Yb-doped fiber laser," Photon. Res. **8**, 246–251 (2020).

35. B. Frisquet, B. Kibler, and G. Millot, "Collision of Akhmediev breathers in nonlinear fiber optics," Phys. Rev. X **3**, 041032 (2013).

36. P. Suret, R. El Koussaifi, A. Tikan, C. Evain, S. Randoux, C. Szwaj, and S. Bielawski, "Single-shot observation of optical rogue waves in integrable turbulence using time microscopy," Nat. Commun. **7**, 13136 (2016).